Bioorganic Chemistry 109 (2021) 104685

Contents lists available at ScienceDirect

Bioorganic Chemistry

journal homepage: www.elsevier.com/locate/bioorg

Design and synthesis of novel 3,4-dihydrocoumarins as potent and selective monoamine oxidase-B inhibitors with the neuroprotection against Parkinson's disease

Li Liu [a,1], Yi Chen [a,1], Rui-Feng Zeng [a], Yun Liu [a,b], Sai-Sai Xie [c,*], Jin-Shuai Lan [a,b,*], Yue Ding [a,b], Yi-Ting Yang [d], Jun Yang [e], Tong Zhang [a,b,*]

[a] School of Pharmacy, Shanghai University of Traditional Chinese Medicine, Shanghai 201203, China
[b] Experiment Center of Teaching & Learning, Shanghai University of Traditional Chinese Medicine, Shanghai 201203, China
[c] National Pharmaceutical Engineering Center for Solid Preparation in Chinese Herbal Medicine, Jiangxi University of Traditional Chinese Medicine, Nanchang 330006, China
[d] Shanghai Seventh People's Hospital, Shanghai 200137, China
[e] Department of Pharmacy, Xiangshan Hospital of Traditional Chinese Medicine, Shanghai 200020, China

ARTICLE INFO

Keywords:
3,4-dihydrocoumarins
*H*MAO-B inhibitors
Neuroprotection
Parkinson's disease
Molecular docking

ABSTRACT

The monoamine oxidase-B (MAO-B) inhibitors with neuroprotective effects are better for Parkinson's disease (PD) treatment, due to the complicated pathogenesis of PD. To develop new *h*MAO-B inhibitors with neuroprotection, a novel series of 3,4-dihydrocoumarins was designed as selective and reversible *h*MAO-B inhibitors to treat PD. Most compounds showed potent and selective inhibition for *h*MAO-B over *h*MAO-A with IC_{50} values ranging from nanomolar to sub-nanomolar. Among them, compound **4d** was the most potent *h*MAO-B inhibitor (IC_{50} = 0.37 nM) being about 20783-fold more active than iproniazid, and exhibited the highest selectivity for *h*MAO-B (SI > 270,270). Kinetic studies revealed that compound **4d** was a reversible and competitive inhibitor of *h*MAO-B. Neuroprotective studies indicated that compound **4d** could protect PC12 cells from the damage induced by 6-OHDA and rotenone. Besides, compound **4d** did not exhibit acute toxicity at a dose up to 2500 mg/kg (po), and could cross the BBB in parallel artificial membrane permeability assay. More importantly, compound **4d** was able to significantly prevent the motor deficits in the MPTP-induced PD model. These results indicate that compound **4d** is an effective and promising candidate against PD.

1. Introduction

Neurodegenerative diseases have attracted extensive attention in recent years, including Parkinson's disease (PD). PD is a debilitating and neurodegenerative disorder, which chiefly occurs in the extrapyramidal system of middle or old age [1]. Although the exact etiology of PD is still unidentified, it is widely supposed that dopamine (DA) depletion is the main reason, and DA depletion is related to the loss of substantia nigra dopaminergic neurons (SNpc), which destroys the balance between the inhibitory neurotransmitter (DA) and excitatory neurotransmitter (acetyl choline) [2]. The main clinical features of PD are motor dysfunctions, such as the static tremor, postural instability and myotonia,

Abbreviations: MAO, Monoamine oxidase; PD, Parkinson's disease; SNpc, substantia nigra dopaminergic neurons; L-DOPA, L-3,4-dihydroxyphenylalanine; COMT, Catechol-O-methyl transferase; H_2O_2, Hydrogen peroxide; ROS, Reactive oxygen species; SAR, Structure–activity relationships; BBB, Blood–brain barrier; ADME, Absorption, distribution, metabolism and excretion; CNS, Central nervous system; MW, Molecular weight; HBA, Hydrogen bond acceptor; HBD, Hydrogen bond donor; tPSA, Topological polar surface area; PAMPA, Parallel artificial membrane permeability assay; MPTP, 1-methyl-4-phenyl-1,2,3,5-tetrahydropyridine; MPP^+, 1-methyl-4-phenylpyridinium; TLC, Thin layer chromatography; PBS, Phosphate buffer solution; MOE, Molecular Operating Environment; PBL, Porcine brain lipid; CMC-Na, Carboxymethyl cellulose sodium.

* Corresponding authors at: School of Pharmacy, Shanghai University of Traditional Chinese Medicine, Shanghai 201203, China (J.-S. Lan and T. Zhang); National Pharmaceutical Engineering Center for Solid Preparation in Chinese Herbal Medicine, Jiangxi University of Traditional Chinese Medicine, Nanchang 330006, China (S.-S. Xie).

E-mail addresses: xiesaisainanchang@hotmail.com (S.-S. Xie), lanjinshuai_shut@126.com (J.-S. Lan), zhangtongshutcm@hotmail.com (T. Zhang).

[1] These authors contributed equally to this work.

https://doi.org/10.1016/j.bioorg.2021.104685
Received 9 June 2020; Received in revised form 13 January 2021; Accepted 22 January 2021
Available online 2 February 2021

generally accompanied with non-motor symptoms including depression and anxiety. The most PD treatment is to increase the DA concentration in the brain using dopaminergic agonists, such as L-3,4-dihydroxyphenylalanine (L-DOPA) [3]. Although L-DOPA is considered to be a useful drug in PD treatment, its serious side effects still limit its application, such as wearing-off, involuntary abnormal movement, dyskinesia and severe motor complications [4]. Other effective therapies include catechol-O-methyl transferase (COMT) and monoamine oxidase (MAO) inhibitors that reduce the metabolism of DA [5].

In addition, oxidative damage has been reported to play a key role in neurodegeneration. Hydrogen peroxide (H_2O_2) and other reactive oxygen species (ROS) from oxidative dehydrogenation of DA catalyzed by MAO may contribute to oxidative stress and cell damage [6]. There are two kinds of MAO in human brain, including *h*MAO-A and *h*MAO-B. Furthermore, the expression level and physiological activity of *h*MAO-B (not *h*MAO-A) is increased with aging, and perhaps associated with the decline of dopaminergic neurons in SNpc [7]. Therefore, the MAO-B inhibitor is able to reduce the DA metabolism to increase DA level, and relieve the oxidative damage, which may slow down the neurodegenerative processes in PD [8]. Among the MAO-B inhibitors, rasagiline and selegiline are used as a monotherapy in early PD. In the late stage of PD, the MAO-B inhibitors are combined with L-DOPA and DA agonist for the adjuvant therapy [9,10]. Nonetheless, as disease modifying drugs, rasagiline and selegiline show no distinct neuroprotective action in the clinical trials, which limit its clinical application [11]. So we hope to develop an effective drug against PD, which not only was a selective and reversible MAO-B inhibitor, but also has a clear neuroprotection, to meet the medical needs of PD.

In the last few years, coumarins has been selected as a promising scaffold to develop potent *h*MAO inhibitors [12]. In particular, coumarins with different substitutes exhibited a selective *h*MAO-B inhibition [13-16]. In our earlier works, a series of coumarins has been reported as selective and potent MAO-B inhibitors [17-19]. However, the selective and potent *h*MAO-B inhibitors based on 3,4-dihydrocoumarins have never been developed. Coumarins and 3,4-dihydrocoumarins have similar structures, so we assume that the simplified 3,4-dihydrocoumarins may improve *h*MAO inhibitory properties. In addition, various molecules with benzyloxy substituted have been reported as novel selective *h*MAO-B inhibitors in recent years, such as indoles, acetophenones, chromones, quinolinones, chromanones, phthalide and α-tetralone analogues [20-26]. To develop an effective *h*MAO-B inhibitor with the neuroprotective activity, the different alkoxy substituents, such as phenylpropoxy, phenylethoxy and benzoxy, were introduced to the 3,4-dihydrocoumarins. To further investigate the structure–activity relationships (SAR) against *h*MAO-A and *h*MAO-B, different substitutions (Br, F, NO_2 and CH_3) were introduced to the benzyloxy ring. Molecular modeling, reversibility and kinetic studies were performed to further investigate their interaction with *h*MAO-B. Moreover, neuroprotective effects of the target compounds were tested in neurotoxins-induced PC12 cells models treated by 6-OHDA and rotenone. To study the drug-like properties, ADMET properties, blood–brain barrier (BBB) permeability and the toxicity of new compounds were also evaluated. Finally, the therapeutic effect of new 3,4-dihydrocoumarin derivates were evaluated using the MPTP-induced motor dysfunction models.

2. Results and discussion

2.1. Chemistry

The target compounds 3,4-dihydrocoumarins **4** were synthesized with a high yield. As shown in Scheme 1, the commercially available compound 7-hydroxy-coumarin (**1**) was efficiently reduced to 7-hydroxychroman-2-one (**2**) in acetic acid with hydrogen and Pd/C at 50 °C [27]. Then, the obtained compound **2** was reacted with the appropriate benzyl bromides (**3**) in the presence of K_2CO_3 in acetonitrile to produce compounds **4** (52–72%). Finally, all target compounds were confirmed by ^1H NMR, ^{13}C NMR and mass spectrometry.

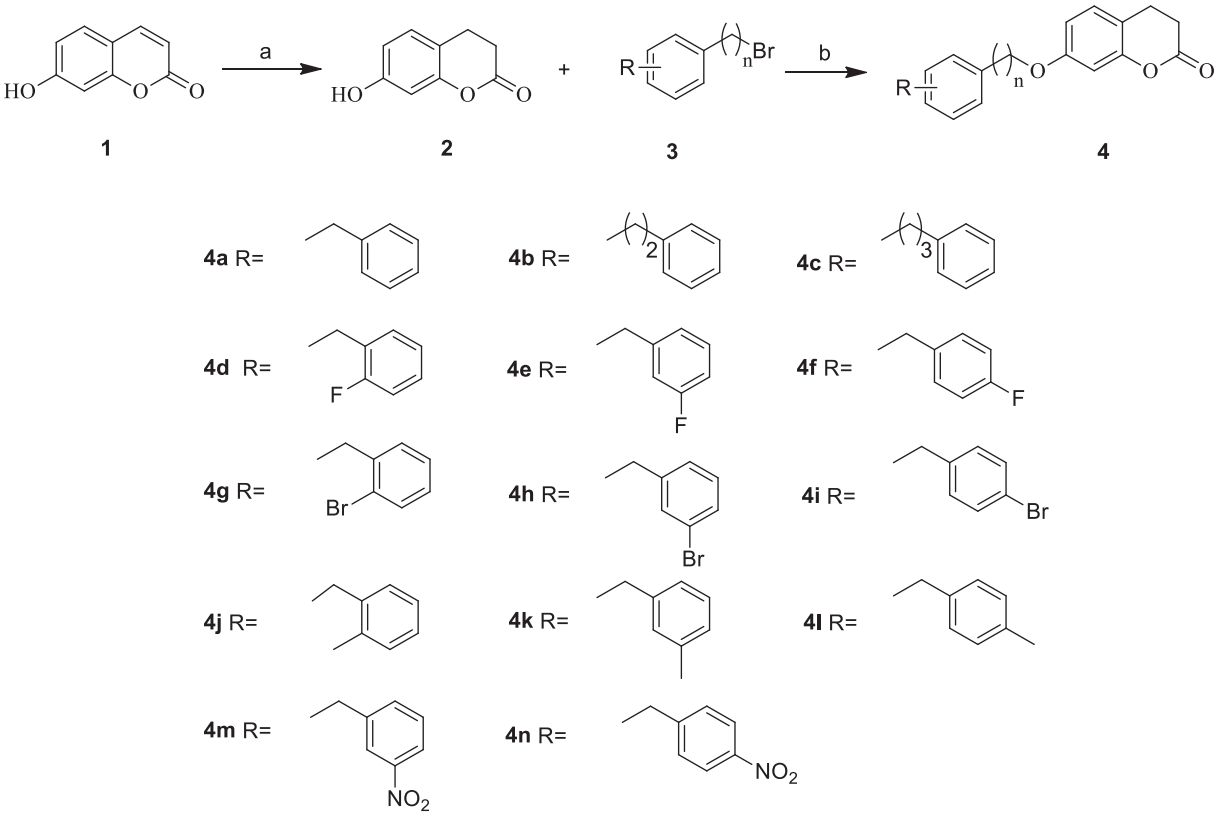

Scheme 1. Syntheses of target compounds **4**. Reagents and conditions: (a) H_2, Pd/C (10%), CH_3COOH, 50 °C, 17 h; (b) K_2CO_3, CH_3CN, reflux, 12 h.

2.2. Effect of MAO inhibition activity

Using iproniazid as a reference, the *h*MAO inhibition of target compounds were evaluated by the Amplex-Red MAO assay [21]. At the same time, the corresponding IC_{50} values of 3,4-dihydrocoumarin derivatives on *h*MAO inhibition were figured out, and the selectivity of *h*MAO-B over *h*MAO-A was also listed (Table 1). The results indicated most 3,4-dihydrocoumarin derivatives showed a potent and selective inhibitory activity to *h*MAO-B with IC_{50} values in the low nanomolar range. Among these derivatives, the most effective inhibitor was compound **4d** (IC_{50} = 0.37 nM for *h*MAO-B), which was approximately 20783-fold more active than that of iproniazid, and exhibited the highest selectivity for *h*MAO-B (SI > 270,270). Interestingly, this finding was inconsistent with the inhibition of rat MAO (*r*MAO) [15], which might be attributed to the difference between *h*MAO and *r*MAO. Although most of 3,4-dihydrocoumarin derivatives showed less *h*MAO-A inhibition, the most potent *h*MAO-A inhibitor compound **4f (**IC_{50} = 5.54 μM) was almost equivalent to iproniazid (IC_{50} = 6.55 μM).

Firstly, introducing groups with different sizes into 7-position of 3,4-dihydrocoumarins, compounds **4a-c** were synthesized. As shown in Table 1, compound **4a** had an IC_{50} value of 1.33 nM for *h*MAO-B. However, the *h*MAO inhibition of compound **2** was remarkably low (IC_{50} > 100 μM), suggesting that the benzyloxy substitute was critical for the inhibitory activity. To extend the length of the side chain with the phenylethoxy and phenylpropoxy, compound **4b** and **4c** were synthesized, but their *h*MAO-B inhibitions were (compound **4b**, IC_{50} = 3.57 nM and compound **4c**, IC_{50} = 4.55 nM) decreased compared with compound **4a**. Based on the above results, we might draw a conclusion that the smaller benzyloxy substitution in 3,4-dihydrocoumarins was more suitable for the substrate/inhibitors binding pockets of *h*MAO-B. Since compound **4a** with a benzyloxy substituent showed a good *h*MAO-B inhibitory activity, it was taken as a lead compound to explore SARs by various substitutions of the 7-benzyloxy group. As shown in the Table 1, the electronic property (CH_3, F, Br and NO_2) and position of the substituents played an important role in *h*MAO-B inhibition. Compared to compound **4a,** the MAO-B inhibition of compound **4d-f** with F substituent was significantly enhanced, and the position of F also had a little effect upon the *h*MAO-B inhibition. For example, **4d** with F substituent at *ortho*-position showed more potent *h*MAO-B inhibition than compounds with F substituent at *meta*-position (compound **4e**) or *para*-position (compound **4f**). However, introducing other electro-withdraw substituents, Br and NO_2, the obtained compounds **4gm** and **4n** exhibited a decrease in *h*MAO-B inhibition, which was perhaps caused by the large sizes and different electron-withdrawing properties. Especially, compound **4i** (IC_{50} = 8.31 nM) with Br substituent reduced the *h*MAO-B inhibition of compound **4a** by 6.2 times. Moreover, the *h*MAO-B inhibition of compound **4h** (IC_{50} = 0.69 nM) was more effective than that of compound **4g** or **4i** with *para*- and *ortho*-substituted. On the other hand, compared with compound **4a**, introduction of an electro-donating substituent, CH_3, to ortho - or *meta*-position (compounds **4j** and **4k**) could also slightly enhanced the inhibition of *h*MAO-B, but compound **4l** with CH_3 in *para*-substitution had a weaker inhibition of *h*MAO-B than that of *meta*- and *ortho*-substituents. Moreover, compounds **4d-f** with F substituent were more potent than that of compound **4j-l** with CH_3 substituent in *h*MAO-B inhibition, further suggesting that the smaller electro-withdraw substituent on the benzyloxy was suitable to inhibit *h*MAO-B.

Table 1
*h*MAO inhibitory activities of the target compounds.

Compounds	n	R	*h*MAO-A IC_{50} (μM)[a]	*h*MAO-B IC_{50} (nM)[a]	Selectivity Index
2	–	–	10.62 ± 0.58%[b]	46.73 ± 2.36%[b]	–
4a	1	–	10.62 ± 0.25%[b]	1.33 ± 0.09	>75187
4b	2	–	45.85 ± 1.03%[b]	3.57 ± 0.09	>28011
4c	3	–	72.29 ± 0.91	4.55 ± 0.08	15,888
4d	1	2-F	29.72 ± 0.53%[b]	0.37 ± 0.04	>270270
4e	1	3-F	38.44 ± 0.26	0.81 ± 0.03	45,457
4f	1	4-F	5.54 ± 0.11	0.67 ± 0.06	8269
4g	1	2-Br	14.56 ± 0.24	3.70 ± 0.16	3935
4h	1	3-Br	32.59 ± 0.38	0.69 ± 0.05	47,232
4i	1	4-Br	26.76 ± 0.81%[b]	8.31 ± 0.21	>12034
4j	1	2-Me	97.48 ± 0.58	0.93 ± 0.14	104,817
4k	1	3-Me	33.61 ± 0.18	1.17 ± 0.13	28,726
4l	1	4-Me	48.33 ± 0.42	2.43 ± 0.06	19,889
4m	1	3-NO_2	18.74 ± 0.22	2.27 ± 0.13	8256
4n	1	4-NO_2	23.89 ± 0.41	3.20 ± 0.08	7466
Iproniazid			6.55 ± 0.24	7,690 ± 280	0.8
Rasagiline			7.65 ± 0.41	40.52 ± 0.37	18.88

[c]Selectivity Index = IC_{50} (MAO-A)/IC_{50} (MAO-B).
[a] IC_{50}: 50% inhibitory concentration (means ± SEM of three experiments).
[b] Test concentration is 100 μM.

2.3. Reversibility of hMAO-B inhibition

To investigate 3,4-dihydrocoumarin derivatives were reversible or irreversible *h*MAO-B inhibitors, the dilution assay was evaluated [28]. Compound **4d** was selected as a representative *h*MAO-B inhibitor duo to its most potent *h*MAO-B inhibition. The recovery of enzymatic activity was evaluated after a dilution of the enzyme-inhibitor complexes, and an irreversible inhibitor (pargyline) was used as a reference. Compound **4d** at concentrations of 0, 10 and 100*IC_{50} was preincubated with *h*MAO-B for 30 min and then obtained concentrations of 0, 0.1 and 1*IC_{50} by diluted 100-fold. For an irreversible inhibitor, the enzyme activity can't recover after diluting the enzyme–inhibitor complex. For a reversible inhibitor, the enzymatic activity is expected to be approximate 90% after dilution to 0.1*IC_{50}, and 50% after dilution to 1*IC_{50}. In the Fig. 1, the *h*MAO-B activities were recovered to 78% of the control (in absence of inhibitor) when compound **4d** was diluted to 0.1*IC_{50}. After dilution of compound **4d** to 1*IC_{50}, the *h*MAO-B activities were recovered to 43%. After a similar incubation of *h*MAO-B with pargyline, the *h*MAO-B activities were not fully recovered (<10% of control). Therefore, these experiments distinctly showed that compound **4d** was a reversible *h*MAO-B inhibitor.

2.4. Kinetic study of hMAO-B inhibition

Compound **4d** was also used to evaluate the type of *h*MAO-B inhibition, which was determined by Michaelis-Menten kinetic experiments

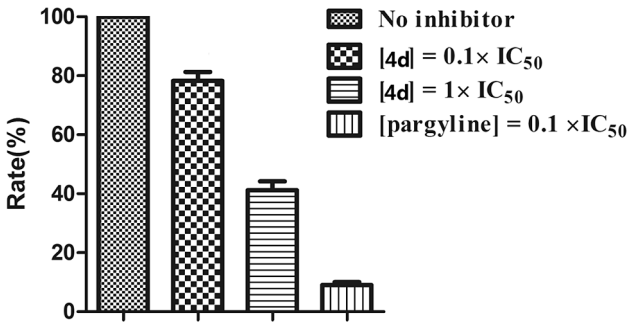

Fig. 1. The reversibility of inhibition of MAO-B by compound **4d**. MAO-B was preincubated with **4d** at 10 × IC_{50} and 100 × IC_{50} for 30 min and then diluted to 0.1 × IC_{50} and 1 × IC_{50}, respectively. For comparison, the irreversible MAO-B inhibitor, (R)-deprenyl, at 10 × IC_{50}, was similarly incubated with MAO-B and diluted to 0.1 × IC_{50}. The residual activity of MAO-B was subsequently measured.

[29]. Five different concentrations of *p*-tyramine (50–1500 μM) were used to measure the catalytic rate, and each graph was constructed at four different concentrations of compound **4d** (0, 0.25, 0.5 and 0.75 nM). The overlapping reciprocal Lineweaver-Burk plots (Fig. 2) exhibited that the graphs of compound **4d** in different concentrations were linear and intersected at the *y*-axis. This pattern suggested that compound **4d** was a competitive *h*MAO-B inhibitor, and this result further proved that compound **4d** was a reversible *h*MAO-B inhibition.

2.5. Molecular modeling studies

In order to explain the *h*MAO-B selectivity of 3,4-dihydrocoumarins, a structure-based molecular modeling study was carried out using the X-ray crystal structures of *h*MAO-A (PDB code 2Z5X) and *h*MAO-B (PDB code 2 V61) [30]. According to the inhibition results, compound **4d** was selected as a typical ligand, and the 2D and 3D pictures of binding modes were shown in Fig. 3. As illustrated in Fig. 3A and 3B, compound **4d** located in the well-known binding pocket of *h*MAO-B, with the 3,4-dihydrocoumarin ring interacting with Lle 198, Leu 171, Gln 206 and Cys 172 at bottom of the substrate cavity, and a hydrogen bond was also formed between the carbonyl oxygen of the ligand and Tyr 435. Moreover, the F-substituted benzyloxy group occupied the entrance cavity, which was a hydrophobic subunit constituted by Tyr 326, Ile 316, Pro 104, Pro 102 and Ile 199. To further prove the importance of the benzyloxy to *h*MAO-B inhibition, compound **2** was also docked with the *h*MAO-B. The result in Fig. S1 showed that compound **2** could only locate in the substrate cavity of *h*MAO-B and no other interaction was established between compound **2** and the *h*MAO-B, suggesting the 3,4-dihydrocoumarin structure alone could not inhibit *h*MAO-B and the benzyloxy substituent was needed for *h*MAO-B inhibition [20-26]. For *h*MAO-A, in Fig. 3C and 3D, it showed no interaction between the *h*MAO-A with the ligands [31,32]. As a result, the *h*MAO-B selectivity could be owed to the hydrogen bond interaction between compound **4d** and *h*MAO-B.

2.6. Cytotoxicity and neuroprotection assays in PC12 cells

To prove the neuroprotection of these 3,4-dihydrocoumarins, the cytotoxicity of represent compounds **4d-f, 4 h** and **4j** were first test in neuroblastoma cells (PC12). The viability was assessed by the MTT [3-(4,5-dimethyl-2-thiazolyl)-2,5-diphenyl-2H-tetrazolium bromide] assay. As exhibited in Fig. 4, the results demonstrated that these compounds showed slight toxicities at 200 μM after 24 h (the viability over 75%), but most of the compounds at 50 μM and 100 μM showed no

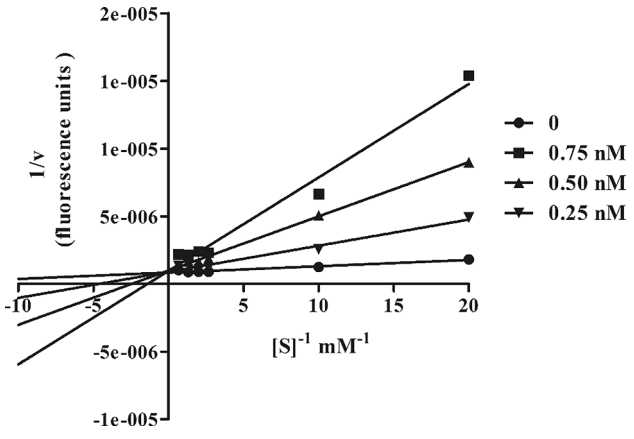

Fig. 2. Kinetic study on the mechanism of *h*MAO-B inhibition by compound **4d**. Overlaid Lineweaver-Burk reciprocal plots of MAO-B initial velocity at increasing substrate concentration (50–1500 μM) in the absence of inhibitor and in the presence of **4d** are shown. Lines were derived from a weighted least-squares analysis of the data points.

neurotoxicity. Then their neuroprotective ability in PC12 cells was also measured by MTT method. PC12 cells were treated with rotenone and 6-OHDA, which is reported to damage cathecolaminergic neurons through ROS generation to generate PD-like models *in vitro* [33]. Rasagiline was used as a positive control. Represent compounds and rasagiline at 10 μM were incubated with PC12 cells for 1 h, then 6-OHDA (200 μM) or rotenone (1.5 μM) were added and incubated with cells for 24 h, and finally the MTT assay was performed to assess the cell viability. As exhibited in Table 2 and Fig. 5A, rasagiline showed a prominent protective effect (34%) at 10 μM concentration in 6-OHDA-treated PC12 cells, which was coincident with literature [11]. All the selected compounds also had significant protective effects on 6-OHDA-induced cells death (>40% protection). In particular, compound **4d** exhibited the highest protection (48% increased) on 6-OHDA-treated cells. As shown in Fig. 5B, all compounds exhibited low neuroprotective activities in rotenone-treated PC12 cells, which was consistent with the rasagiline. Compounds **4d** and **4h** had the best neuroprotection in rotenone-induced cell death (17% increased).

2.7. ADMET prediction.

If a compound wants to be developed as a candidate drug, low toxicities and high pharmacological activities are not enough, and pharmacokinetic profiles of new drug candidates should be assessed as early as possible. Fortunately, the combinatorial chemistry could easily assess the absorption, distribution, metabolism and excretion (ADME) as soon as possible [34]. Online Molinspiration property program was used to calculate ADME properties of compounds **4a-n** [35]. The stipulation of ADME demands that an oral drug should be no more than one violation. Meanwhile, the capability of compounds to cross the blood–brain barrier (BBB) is also essential to develop the central nervous system (CNS) drugs [36]. Log BB was calculated for latent applications in brains and defined by the Lipinski's rules: the small polar surface area<90 $Å^2$, the calculated logarithm of the octanol–water partition coefficient (Clog P) <5, the molecular weight (MW) <500, the number of hydrogen bond acceptor (HBA) atoms<10 and the number of hydrogen bond donor (HBD) atoms<5. The log BB is calculated as the following equation: log BB = 0.0148 × PSA + 0.152 × Clog P + 0.130.

As shown in Table 3, the theoretical calculations of ADME parameters (log P, molecular weight, number of hydrogen donors, topological polar surface area (tPSA), number of rotatable bonds and volume, number of hydrogen acceptors) were presented, and the cases violating Lipinski's law were listed [37]. As indicated by the data, all compounds showed a good ability to cross the BBB and followed the Lipinski's rule with no more than one violate. Thus, the new compounds perhaps had a satisfying pharmacokinetics profile, which further strengthened the biological importance of these compounds.

2.8. In vitro blood–brain barrier permeation assay

The ability to permeate the BBB is vital in PD treatment. The BBB penetration of the target compounds were determined by the parallel artificial membrane permeability assay (PAMPA-BBB), which was described by Pardridge *et al* [36]. Compared with their reported values, the experimental permeability of 9 reference drugs was rectified (Table 4), which presented a good linear correlation: P_e(exp) = 1.0121P_e(Bibl.) – 0.5774 (R^2 = 0.9441). To permeate BBB, compounds were classified as follows: compounds with P_e (10^{-6} cm s^{-1}) > 3.47 for high BBB permeation (CNS +), compounds with P_e (10^{-6} cm s^{-1}) < 1.45 for low BBB permeation (CNS-), and compounds with 3.47 > P_e (10^{-6} m s^{-1}) > 1.45 for uncertain BBB permeation (CNS ±). In Table 5, the P_e values of selected compounds showed that compounds **4d-f**, **4h** and **4j** might have the ability to pass BBB.

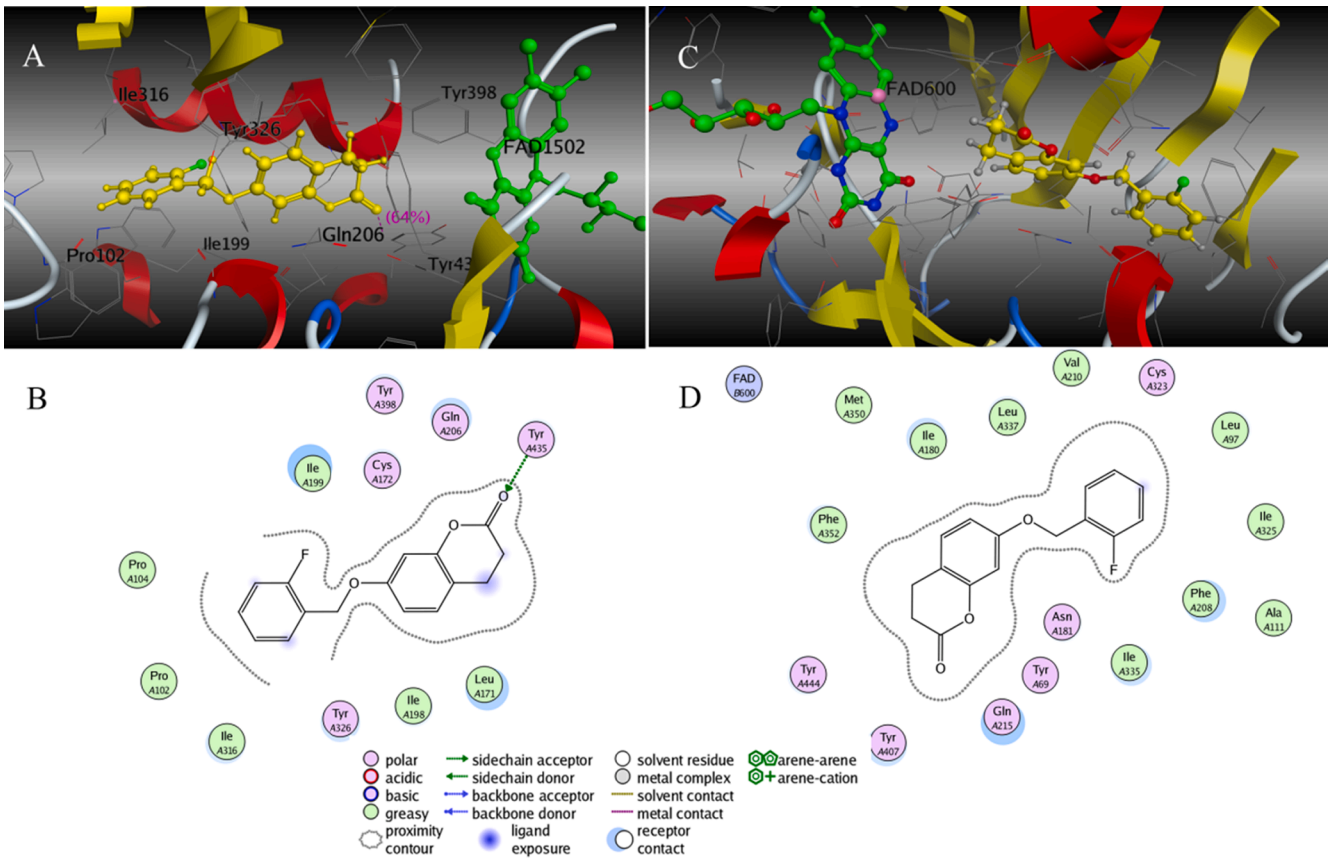

Fig. 3. (A) 3D docking model of compound **4d** with *h*MAO-B. Atom colors: yellow-carbon atoms of compound **4d**, gray-carbon atoms of residues of *h*MAO-B, dark blue-nitrogen atoms, red-oxygen atoms. The dashed lines represent the interactions between the protein and the ligand. (B) 2D schematic diagram of docking model of compound **4d** with *h*MAO-B. (C) 3D docking model of compound **4d** with *h*MAO-A. (D) 2D schematic diagram of docking model of compound **4d** with *h*MAO-A. (For interpretation of the references to colour in this figure legend, the reader is referred to the web version of this article.)

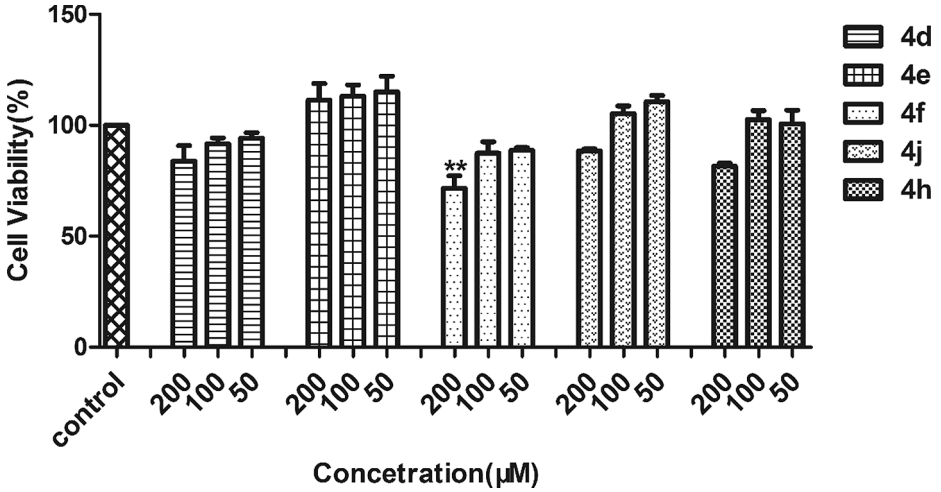

Fig. 4. Effects of compounds **4d**, **4e**, **4f**, **4j** and **4h** on cell viability in PC12 cells. The cell viability was determined by the MTT assay after 24 h of incubation with various concentrations. The results were expressed as a percentage of control cells. Values were reported as the mean ± SD of three independent experiments. $^{**}p < 0.01$ compared to control.

Table 2
Effect of compounds (10 μM) on the survival of PC 12 cells after 6-OHDA and rotenone treatment.

Compound	% survival[a]	
	6-OHDA	rotenone
4d	148.47 ± 9.04***	117.46 ± 7.55**
4e	140.42 ± 5.60***	104.40 ± 3.87
4f	139.43 ± 5.27***	115.58 ± 6.99*
4h	142.18 ± 7.93***	117.66 ± 2.87**
4j	141.34 ± 8.75***	107.64 ± 3.36
control	100	100
Rasagiline	134.07 ± 4.94***	105.59 ± 4.03

[a] Survival data are expressed as the percentage of 6-OHDA- and rotenone-treated cells. Symbols represent significant changes from 6-OHDA- and rotenone-treated cells (*$P < 0.05$; **$P < 0.01$; ***$P < 0.001$), respectively. All data are the means ± SD of at least six values measured in two independent plates.

2.9. Acute toxicity test in vivo

Acute toxicity studies were conducted according to similar reports [38]. After administration of compound **4d** (2,000 mg/kg), any mortality changes and abnormal behavior of mice were monitored constantly for the first 4 h, intermittently for the next 24 h, which continued for 14 days. As shown in Fig. 6, no acute toxicity, including the mortality or body weight reduction, even any obvious abnormal changes in food or water consumption, was observed during the experimental period. Moreover, no mice sacrificed on the 14th day after drug administration, which suggested that compound **4d** was nontoxic.

2.10. Therapeutic effect on parkinsonian motor symptom in the MPTP-induced model

Encouraged by compound **4d** with the MAO-B inhibition and neuroprotective effects *in vitro*, the efficacy of compound **4d** on PD was tested by a MPTP-induced animal model, which was one of wide animal models for PD. Previous studies have demonstrated that in glial cells the MAO-B could convert MPTP (1-methyl-4-phenyl-1,2,3,5-

Table 3
Physical properties of compounds **4a-n**.

Compounds	MW [a]	Clog P [a]	HBA [a]	HBD [a]	PSA [a]	Log BB [a]
4a	254.09	3.483	3	0	35.53	1.185
4b	268.11	3.812	3	0	35.53	1.235
4c	282.13	4.191	3	0	35.53	1.293
4d	272.08	3.626	3	0	35.53	1.207
4e	272.08	3.626	3	0	35.53	1.207
4f	272.08	3.626	3	0	35.53	1.207
4g	332.00	4.346	3	0	35.53	1.316
4h	332.00	4.346	3	0	35.53	1.316
4i	332.00	4.346	3	0	35.53	1.316
4j	268.11	3.982	3	0	35.53	1.261
4k	268.11	3.982	3	0	35.53	1.261
4l	268.11	3.982	3	0	35.53	1.261
4m	299.08	3.226	5	0	87.34	1.913
4n	299.08	3.226	5	0	87.34	1.913
Rules	≤450	≤5.0	≤10	≤5	≤90	≥-1.0

[a] MW: molecular weight; C log P: calculated logarithm of the octanol–water partition coefficient; HBA: hydrogen-bond acceptor atoms; HBD: hydrogen-bond donor atoms; PSA: polar surface area; log BB = 0.0148 × PSA + 0.152 × Clog P + 0.130.

Table 4
Permeability ($Pe \times 10^{-6}$ cm s^{-1}) in the PAMPA-BBB assay for 9 commercial drugs, used in the experiment validation.

Commercial drugs	Bibl[a]	PBS:EtOH (70:30)[b]
Testosterone	17	18.03
Verapamil	16	14.28
beta-Estradiol	12	13.95
Progesterone	9.3	5.97
corticosterone	5.1	3.29
Piroxicam	2.5	1.87
Hydrocortisone	1.9	2.53
Ofloxacin	0.8	0.36
Dopamine	0.2	0.11

[a] Taken from Ref. [37].
[b] Data are the mean ± SD of three independent experiments.

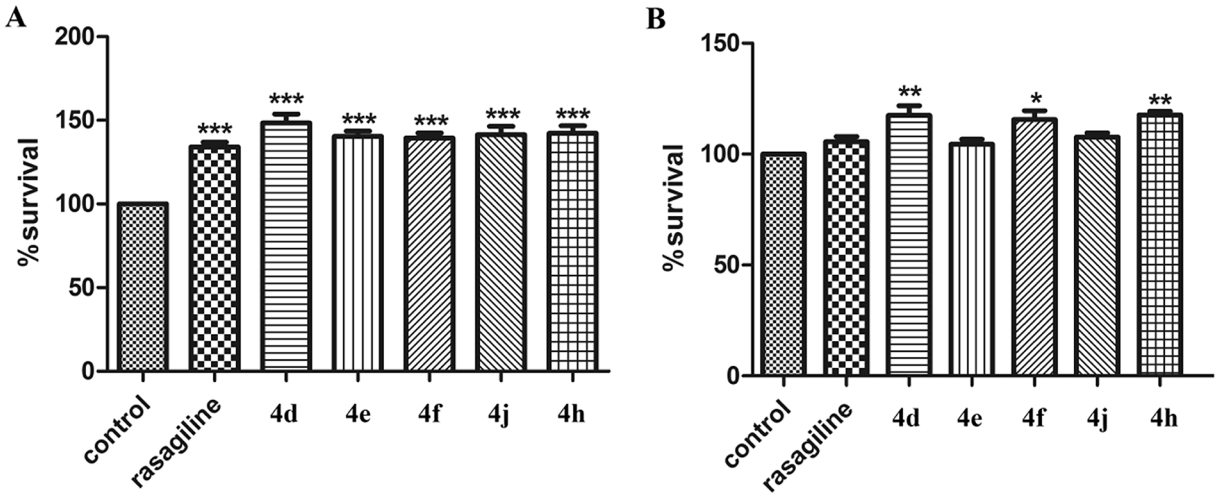

Fig. 5. Neuroprotective effects of compounds **4d**, **4e**, **4f**, **4j** and **4h** against 6-OHDA (A) and rotenone-induced toxicity (B) in PC12 cells. Rasagiline was used as the reference compound. Results are expressed as percent viability compared to cells not treated with compounds. All data were the means ± SEM of at least five values measured in two independent plates (*$P < 0.05$, **$P < 0.01$).

Table 5
Permeability ($P_e \times 10^{-6}$ cm s^{-1}) in the PAMPA-BBB assay for novel 3,4-dihydrocoumarins derivatives and their predictive penetration in the CNS.

Compound	$Pe \times 10^{-6}$ cm s^{-1}	Prediction
4d	12.9 ± 0.6	CNS+
4e	10.4 ± 0.5	CNS+
4f	13.6 ± 0.8	CNS+
4h	11.9 ± 0.1	CNS+
4j	12.7 ± 0.6	CNS+

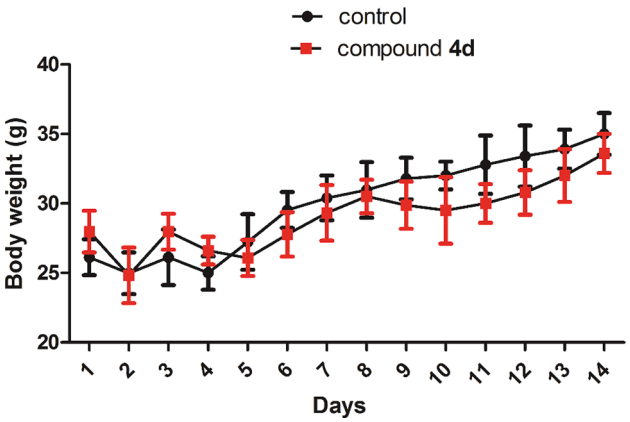

Fig. 6. Effects on body weight of mice fed compound **4d** in the acute toxicity test.

tetrahydropyridine) to neurotoxin MPP^+ (1-methyl-4- phenylpyridinium) [39]. In brain SNPC, MPP^+ leads to the death of dopaminergic neurons, resulting in permanent motor symptoms in PD. After MPTP administration, mice were orally administered compound **4d** and rasagiline (a positive control) for 3 consecutive days. Hind limb and rotarod tests were used to evaluate the behaviors of mice, which was aimed to estimate if compound **4d** could cure the motor symptoms induced by MPTP [40,41]. As demonstrated in Fig. 7A, the MPTP-treated mice exhibited a bad postural balance, with an average score of 2.1 compared to 4.0 of the control. In contrast, the mice treated with rasagiline (10 mg/kg) showed a great improvement, getting an average score of 3.8. Surprisingly, after treatment with compound **4d** (5 or 10 mg/kg), the score of mice were also improved, especially in group of 10 mg/kg. As shown in Fig. 7B, MPTP obviously decreased the latency to fall from the rotarod (118 *sec*), but the decrement of latency was significantly lower in the compound **4d**-treated mice (196 *sec* in 5 mg/kg and 285 *sec* in 10 mg/kg). To summarize, compound **4d** could effectively prevent the motor deficits, which associated with PD.

3. Conclusions

As indicated in our studies, a series of 3,4-dihydrocoumarin derivatives can be considered as remarkably selective and competitive *h*MAO-B inhibitors, even compared to the previous coumarin derivatives. The results also exhibited that most compounds were potent and reversible inhibitors of *h*MAO-B rather than *h*MAO-A. From the primary SAR of the synthesized compounds, we can know that the size of benzyloxy substitution of 3,4-dihydrocoumarins was more fitting for volume of the substrate/inhibitors binding pockets, and the small electron-withdrawing groups on the benzyloxy ring were more suitable for *h*MAO-B inhibitory activity. When estimated the ADMET properties in silico, the target compounds exhibited the good oral absorption and good BBB permeability. In addition, these compounds also exhibited neuroprotective properties in PC12 cells treated with 6-OHDA or rotenone *in vitro*. Among them, compound **4d** had a significant protection on DAergic neurons from cytotoxic damage *in vitro*, and reduced PD-associated motor deficits in MPTP-induced PD model. Based on the high encouraging results, further studies are needed to confirm the roles of these compounds to against PD.

4. Experimental section

4.1. Chemistry

All of chemicals (reagent grade) were used from Sino pharm Chemical Reagent Co., Ltd. (China). Analytical thin layer chromatography (TLC) on precoated silica gel GF254 (Qingdao Haiyang Chemical Plant, Qing-Dao, China) plates were used to monitored reaction progress and the spots were detected under UV light (254 nm). On a BRUKER AVANCE III spectrometer at 25 °C, ^{1}H NMR and ^{13}C NMR spectra were measured and referenced to TMS. Chemical shifts were reported in ppm (δ) using the residual solvent line as internal standard. Splitting patterns were designed as s, singlet; d, doublet; t, triplet; m, multiplet. Mass spectra were obtained on a MS Agilent 1100 Series LC/MSD Trap mass spectrometer (ESI-MS).

4.2. General procedures for the preparation of compound 4

Compound **2** was synthesized based on the reported method [26]. The commercial 7-hydroxy-coumarin (**1**) was dissolved in acetic acid, and a catalytic amount of Pd/C was added to the mixture. The solution was stirred at 50 °C in H_2 atmosphere for 17 h. After the reaction was completed, the catalyst was eliminated by filtering to get a crude product, which was recrystallized for further purification and obtained the desired in a yield of 90%.

Then, compound **2** (1.85 mmol) was suspended in acetonitrile (15

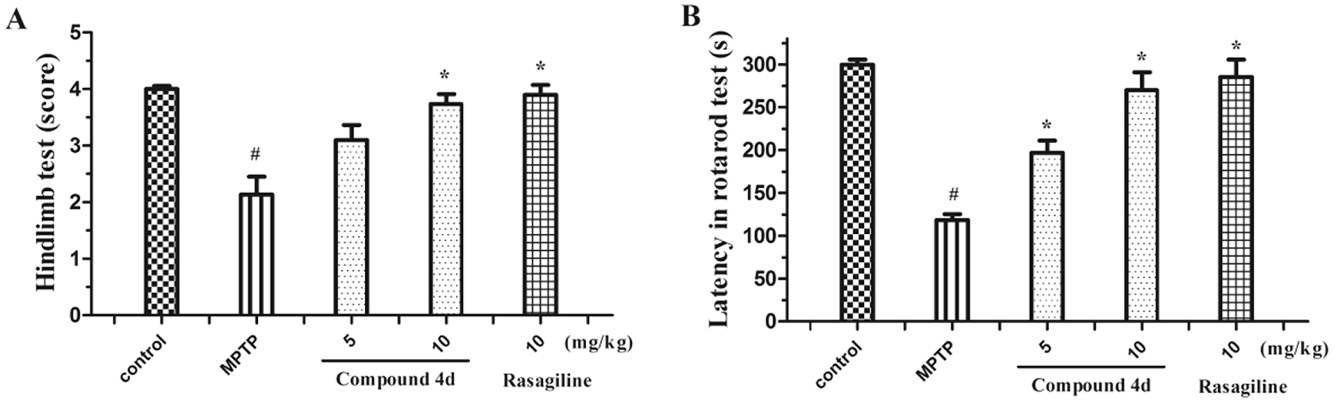

Fig. 7. Compound **4d** alleviates motor deficits in MPTP-induced PD mice. (A) The score of the hindlimb test; (B) The latency of mice to fall down from the rotarod. # $p < 0.05$, compared to control group; * $p < 0.05$ compared to MPTP group.

mL) containing K_2CO_3 (3.70 mmol). The reaction was treated with a properly substituted arylalkyl bromide **3** (2.04 mmol) and heated for 12 h under reflux. After the reaction completed, the acetonitrile was evaporated *in vacuo* and the mixture was then poured into water, which was extracted with 100 mL of EtOAc for 3 times, washed with brine, dried over anhydrous Na_2SO_4 and purified by chromatography (petroleum ether/EtOAc) on *silica gel* to get compound **4**.

4.2.1. 7-(benzyloxy)chroman-2-one (4a)

Compound **2** was reacted with compound **3a** following the general procedure to give compound **4a** as a yellow oil (68% yield); ^{1}H NMR (400 MHz, $CDCl_3$) δ 7.44 –7.30 (m, 5H), 7.08 (d, J = 8.3 Hz, 1H), 6.73 (dd, J = 8.3, 2.5 Hz, 1H), 6.68 (d, J = 2.5 Hz, 1H), 5.05 (s, 2H), 2.93 (t, J = 7.2 Hz, 2H), 2.77 (dd, J = 8.4, 6.2 Hz, 2H). ^{13}C NMR (100 MHz, $CDCl_3$) δ 168.60, 158.77, 152.67, 136.49, 128.67, 128.67, 128.48, 128.14, 127.46, 127.46, 114.69, 111.36, 103.58, 70.31, 29.46, 23.03; ESI-MS: 255.3 $[M + H]^+$.

4.2.2. 7-(phenethoxy)chroman-2-one (4b)

Compound **2** was reacted with compound **3b** following the general procedure to give compound **4b** as a yellow oil (58% yield); ^{1}H NMR (400 MHz, $CDCl_3$) δ 7.32 – 7.27 (m, 5H), 7.06 (d, J = 8.3 Hz, 1H), 6.64 (dd, J = 8.3, 2.5 Hz, 1H), 6.61 (d, J = 2.5 Hz, 1H), 4.14 (dd, J = 7.1, 3.9 Hz, 2H), 2.93 (t, J = 7.2 Hz, 2H), 2.80 – 2.75 (m, 2H), 2.74 –2.61 (dd, J = 11.2, 4.7 Hz, 2H). ^{13}C NMR (100 MHz, $CDCl_3$) δ 168.64, 158.87, 152.78, 138.00, 128.99, 128.99, 128.54, 128.54, 128.47, 126.60, 114.48, 111.02, 103.27, 68.95, 35.36, 29.71, 23.02; ESI-MS: 269.3 $[M + H]^+$.

4.2.3. 7-(3-phenylpropoxy)chroman-2-one (4c)

Compound **2** was reacted with compound **3c** following the general procedure to give compound **4c** as a yellow oil (58% yield); ^{1}H NMR (400 MHz, $CDCl_3$) δ 7.28 (m, 1H), 7.22 – 7.19 (m, 3H), 6.97 (d, J = 8.2 Hz, 1H), 6.68 – 6.57 (m, 1H), 6.42 (m, 2H), 3.92 (dd, J = 6.3, 3.8 Hz, 2H), 2.88 – 2.69 (m, 6H), 2.11 – 2.06 (m, 2H). ^{13}C NMR (100 MHz, $CDCl_3$) δ 179.13, 159.04, 154.88, 141.54, 128.52, 128.52, 128.46, 128.42, 128.42, 126.02, 111.04, 107.40, 103.15, 67.27, 34.76, 29.51, 23.92, 23.01; ESI-MS: 283.3 $[M + H]^+$.

4.2.4. 7-((2-fluorobenzyl)oxy)chroman-2-one (4d)

Compound **2** was reacted with compound **3d** following the general procedure to give compound **4d** as a yellow oil (72% yield); ^{1}H NMR (400 MHz, $CDCl_3$) δ 7.48 (m, 1H), 7.32 (m, 1H), 7.17 (td, J = 7.5, 1.0 Hz, 1H), 7.10 (dt, J = 8.6, 1.8 Hz, 2H), 6.74 (dd, J = 8.3, 2.5 Hz, 1H), 6.70 (d, J = 2.5 Hz, 1H), 5.11 (s, 2H), 2.94 (t, J = 7.2 Hz, 2H), 2.77 (dd, J = 8.2, 6.0 Hz, 2H). ^{13}C NMR (100 MHz, $CDCl_3$) δ 168.50, 160.47 (d, $^1J_{CF}$ = 245.38 Hz), 158.54, 152.71, 129.91 (d, $^3J_{CF}$ = 8.61 Hz), 129.70, 128.53, 124.33, 123.61, 115.45(d, $^2J_{CF}$ = 21.58 Hz), 114.95, 111.16, 103.66, 64.07, 29.44, 23.04; ESI-MS: 273.3 $[M + H]^+$.

4.2.5. 7-((3-fluorobenzyl)oxy)chroman-2-one (4e)

Compound **2** was reacted with compound **3e** following the general procedure to give compound **4e** as a yellow oil (68% yield); ^{1}H NMR (400 MHz, $CDCl_3$) δ 7.35 (td, J = 7.9, 5.9 Hz, 1H), 7.16 (dd, J = 17.4, 8.4 Hz, 2H), 7.09 (d, J = 8.4 Hz, 1H), 7.04 – 6.97 (m, 1H), 6.72 (dd, J = 8.3, 2.5 Hz, 1H), 6.66 (d, J = 2.5 Hz, 1H), 5.04 (s, 2H), 2.94 (t, J = 7.2 Hz, 2H), 2.77 (t, J = 7.2 Hz, 2H). ^{13}C NMR (100 MHz, $CDCl_3$) δ 168.51, 163.02 (d, $^1J_{CF}$ = 245.32 Hz), 158.45, 152.70, 139.13 (d, $^3J_{CF}$ = 7.86 Hz), 130.23 (d, $^3J_{CF}$ = 8.28 Hz), 128.57, 122.70, 115.09, 114.92 (d, $^3J_{CF}$ = 9.03 Hz), 114.19 (d, $^2J_{CF}$ = 22.58 Hz), 111.32, 103.56, 69.46, 29.42, 23.02; ESI-MS: 273.3 $[M + H]^+$.

4.2.6. 7-((4-fluorobenzyl)oxy)chroman-2-one (4f)

Compound **2** was reacted with compound **3f** following the general procedure to give compound **4f** as a yellow oil (68% yield); ^{1}H NMR (400 MHz, $CDCl_3$) δ 7.39 (dd, J = 8.6, 5.4 Hz, 2H), 7.12–7.04 (m, 3H), 6.71 (dd, J = 8.3, 2.5 Hz, 1H), 6.66 (d, J = 2.5 Hz, 1H), 5.00 (s, 2H), 2.94 (t, J = 7.2 Hz, 2H), 2.77 (t, J = 7.2 Hz, 2H). ^{13}C NMR (100 MHz, $CDCl_3$) δ 168.50, 162.56 (d, $^1J_{CF}$ = 245.62 Hz), 158.58, 152.69, 132.26, 129.34, 129.34 (d, $^3J_{CF}$ = 9.17 Hz), 128.53, 115.59, 115.59 (d, $^2J_{CF}$ = 22.57 Hz), 114.85, 111.33, 103.55, 69.64, 29.44, 23.03; ESI-MS: 273.3 $[M + H]^+$.

4.2.7. 7-((2-bromobenzyl)oxy)chroman-2-one (4g)

Compound **2** was reacted with compound **3g** following the general procedure to give compound **4g** as a yellow oil (65% yield); ^{1}H NMR (400 MHz, $CDCl_3$) δ 7.51 (d, J = 8.4 Hz, 2H), 7.29 (d, J = 8.4 Hz, 2H), 7.08 (d, J = 8.3 Hz, 1H), 6.70 (dd, J = 8.3, 2.5 Hz, 1H), 6.65 (d, J = 2.5 Hz, 1H), 5.00 (s, 2H), 2.94 (t, J = 7.2 Hz, 2H), 2.77 (t, J = 7.2 Hz, 2H). ^{13}C NMR (100 MHz, $CDCl_3$) δ 168.46, 158.46, 152.70, 135.53, 131.80, 131.80, 129.05, 129.05, 128.55, 122.06, 114.94, 111.31, 103.58, 69.53, 29.42, 23.03; ESI-MS: 334.2 $[M + H]^+$.

4.2.8. 7-((3-bromobenzyl)oxy)chroman-2-one (4h)

Compound **2** was reacted with compound **3h** following the general procedure to give compound **4h** as a yellow oil (67% yield); ^{1}H NMR (400 MHz, $CDCl_3$) δ 7.58 (s, 1H), 7.46 (d, J = 7.9 Hz, 1H), 7.34 (d, J = 7.9 Hz, 1H), 7.27 (d, J = 7.9 Hz, 1H), 7.09 (d, J = 8.3 Hz, 1H), 6.71 (dd, J = 8.3, 2.5 Hz, 1H), 6.66 (d, J = 2.5 Hz, 1H), 5.01 (s, 2H), 2.94 (t, J = 7.2 Hz, 2H), 2.77 (t, J = 7.2 Hz, 2H). ^{13}C NMR (100 MHz, $CDCl_3$) δ 168.47, 158.43, 152.71, 138.84, 131.20, 130.30, 130.22, 128.58, 125.81, 122.77, 115.01, 111.30, 103.56, 69.37, 29.42, 23.03; ESI-MS: 334.2 $[M + H]^+$.

4.2.9. 7-((4-bromobenzyl)oxy)chroman-2-one (4i)

Compound **2** was reacted with compound **3i** following the general procedure to give compound **4i** as a yellow oil (68% yield); ^{1}H NMR (400 MHz, $CDCl_3$) δ 7.57 (d, J = 7.3 Hz, 1H), 7.52 (d, J = 7.3 Hz, 1H), 7.32 (t, J = 7.0 Hz, 1H), 7.18 (t, J = 7.0 Hz, 1H), 7.00 (d, J = 9.1 Hz, 1H), 6.57 – 6.50 (m, 2H), 5.08 (s, 2H), 2.84 (t, J = 6.3 Hz, 2H), 2.73 (t, J = 6.3 Hz, 2H). ^{13}C NMR (100 MHz, $CDCl_3$) δ 167.66, 158.47, 155.00, 136.34, 132.60, 131.11, 129.19, 128.87, 127.56, 119.69, 111.22, 107.62, 103.65, 69.47, 29.71, 23.91; ESI-MS: 334.2 $[M + H]^+$.

4.2.10. 7-((2-methylbenzyl)oxy)chroman-2-one (4j)

Compound **2** was reacted with compound **3j** following the general procedure to give compound **4j** as a yellow oil (58% yield); ^{1}H NMR (400 MHz, $CDCl_3$) δ 7.38 (d, J = 7.0 Hz, 1H), 7.25–7.20 (m, 2H), 7.09 (d, J = 8.3 Hz, 1H), 6.74 (dd, J = 8.3, 2.5 Hz, 1H), 6.70 (d, J = 2.5 Hz, 1H), 5.01 (s, 2H), 2.94 (t, J = 7.2 Hz, 2H), 2.77 (t, J = 7.2 Hz, 2H), 2.37 (s, 3H). ^{13}C NMR (100 MHz, $CDCl_3$) δ 168.02, 158.38, 152.15, 136.15, 133.75, 129.96, 128.06, 127.95, 125.55, 114.15, 110.74, 102.95, 68.40, 28.93, 22.50, 18.33; ESI-MS: 269.3 $[M + H]^+$.

4.2.11. 7-((3-methylbenzyl)oxy)chroman-2-one (4k)

Compound **2** was reacted with compound **3a** following the general procedure to give compound **4a** as a yellow oil (60% yield); ^{1}H NMR (400 MHz, $CDCl_3$) δ 7.30 – 7.19 (m, 4H), 7.14 (d, J = 7.4 Hz, 1H), 7.08 (d, J = 8.3 Hz, 1H), 6.73 (dd, J = 8.3, 2.5 Hz, 1H), 6.68 (d, J = 2.5 Hz, 1H), 5.00 (s, 2H), 2.93 (t, J = 7.2 Hz, 2H), 2.77 (t, J = 7.2 Hz, 2H), 2.37 (s, 3H). ^{13}C NMR (100 MHz, $CDCl_3$) δ 168.60, 158.84, 152.66, 138.39, 136.39, 128.91, 128.57, 128.46, 128.21, 124.57, 114.62, 111.36, 103.56, 70.39, 29.47, 23.03, 21.42; ESI-MS: 269.3 $[M + H]^+$.

4.2.12. 7-((4-methylbenzyl)oxy)chroman-2-one (4l)

Compound **2** was reacted with compound **3l** following the general procedure to give compound **4l** as a yellow oil (66% yield); ^{1}H NMR (400 MHz, $CDCl_3$) δ 7.30 (d, J = 8.0 Hz, 2H), 7.19 (d, J = 8.0 Hz, 2H), 7.07 (d, J = 8.3 Hz, 1H), 6.72 (dd, J = 8.3, 2.5 Hz, 1H), 6.67 (d, J = 2.5 Hz, 1H), 5.00 (s, 2H), 2.93 (t, J = 7.2 Hz, 2H), 2.76 (t, J = 7.2 Hz, 2H), 2.36 (s, 3H). ^{13}C NMR (100 MHz, $CDCl_3$) δ 168.59, 158.83, 152.65, 137.96, 133.44, 129.34, 129.34, 128.43, 127.60, 127.60, 114.57, 111.37, 103.58, 70.26, 29.48, 23.04, 21.21.

4.2.13. 7-((3-nitrobenzyl)oxy)chroman-2-one (**4m**)

Compound **2** was reacted with compound **3m** following the general procedure to give compound **4m** as a yellow oil (52% yield); ^{1}H NMR (400 MHz, $CDCl_3$) δ 8.31 (s, 1H), 8.20 (d, J = 8.2 Hz, 1H), 7.76 (d, J = 7.7 Hz, 1H), 7.58 (t, J = 7.7 Hz, 1H), 7.12 (d, J = 8.4 Hz, 1H), 6.74 (dd, J = 8.4, 2.5 Hz, 1H), 6.67 (d, J = 2.5 Hz, 1H), 5.14 (s, 2H), 2.95 (t, J = 7.2 Hz, 2H), 2.78 (t, J = 7.2 Hz, 2H). ^{13}C NMR (100 MHz, $CDCl_3$) δ 168.34, 158.10, 152.76, 148.51, 138.73, 133.08, 129.68, 128.73, 123.08, 122.14, 115.38, 111.28, 103.54, 68.94, 29.37, 23.04; ESI-MS: 300.3 $[M + H]^+$.

4.2.14. 7-((4-nitrobenzyl)oxy)chroman-2-one(**4n**)

Compound **2** was reacted with compound **3n** following the general procedure to give compound **4n** as a yellow oil (56% yield); ^{1}H NMR (400 MHz, $CDCl_3$) δ 8.25 (d, J = 8.8 Hz, 2H), 7.60 (d, J = 8.8 Hz, 2H), 7.11 (d, J = 8.3 Hz, 1H), 6.72 (dd, J = 8.3, 2.5 Hz, 1H), 6.66 (d, J = 2.5 Hz, 1H), 5.16 (s, 2H), 2.95 (t, J = 7.2 Hz, 2H), 2.78 (t, J = 7.2 Hz, 2H). ^{13}C NMR (100 MHz, $CDCl_3$) δ 168.30, 158.06, 152.77, 147.68, 143.95, 128.73, 127.62, 127.62, 123.90, 123.90, 115.40, 111.20, 103.56, 68.93, 29.36, 23.03; ESI-MS: 300.3 $[M + H]^+$.

4.3. Biological activity

4.3.1. In vitro inhibition of monoamine oxidase

*h*MAO-A and *h*MAO-B were purchased from Sigma-Aldrich. The MAO-A and MAO-B inhibition of test compounds were assessed by the Amplex Red assay [20]. Briefly, 0.1 mL of sodium phosphate buffer (0.05 M, pH 7.4) containing the test drugs at various concentrations and adequate amounts of recombinant *h*MAO-A or *h*MAO-B required and adjusted to obtain the same reaction velocity, i.e., to oxidize (in the control group) the same concentration of substrate: 165 pmol of *p*-tyramine/min (*h*MAO-A: 1.1 μg protein; specific activity: 150 nmol of *p*-tyramine oxidized to *p*-hydroxyphenylacetaldehyde/min/mg protein; *h*MAO-B: 7.5 μg protein; specific activity: 22 nmol of *p*-tyramine transformed/min/mg protein) were incubated for 15 min at 37 °C in a flat-black-bottom 96-well microtest plate which placed in a dark fluorimeter chamber. After this incubation period, the reaction was started by adding 200 μM (final concentrations) Amplex Red reagent, 1 U/mL horseradish peroxidase and 1 mM *p*-tyramine. The production of H_2O_2 and resorufin were quantified at 37 °C in a SpectraMax Paradigm (Molecular Devices, Sunnyvale, CA) multi-mode detection platform reader based on the fluorescence generated (excitation: 545 nm; emission: 590 nm). The specific fluorescence emission was calculated after subtracting the background activity. The background activity was determined from wells containing all components except the *h*MAO isoforms, which were replaced by a sodium phosphate buffer solution (PBS) (0.05 M, pH 7.4). The percent inhibition was calculated by the following formula: $(1 - IFi/IFc) \times 100$. IFi and IFc were the fluorescence intensities obtained for *h*MAO in the presence and absence of inhibitors after subtracting the respective background.

4.3.2. Reversibility and irreversibility study

The reversibility of *h*MAO-B inhibition was determined by a dilution assay [27]. At concentrations equal to 10 * IC_{50} and 100 * IC_{50} for *h*MAO-B inhibition, compound **4d** was incubated with the enzyme (0.75 mg/ml) for 30 min at 37 °C in PBS (0.05 M, pH 7.4). The parallel control was conducted with buffer instead of compound and the corresponding amount of DMSO was added into all culture medium as co-solvent. After the incubation period, the complex was diluted 100-fold to obtain final concentrations of compound **4d** equal to 0.1 * IC_{50} and 1 * IC_{50}. For comparison, pargyline were incubated with *h*MAO-B at concentrations of 10 * IC_{50} in similar manner and diluted to 0.1 * IC_{50}. The catalytic activity of residual enzyme catalytic rates was determined following the method for the IC_{50} determination and all results were expressed as mean ± SD.

4.3.3. Kinetic study of hMAO-B inhibition

To obtain of the mechanism of action **4d**, reciprocal plots of 1/velocity versus 1/substrate were constructed at different concentrations of the substrate *p*-tyramine (50–3000 μM). Four different concentrations of **4d** (0, 0.25, 0.50 and 0.75 nM) were selected to analyze the inhibition kinetics of *h*MAO-B. The plots were assessed by a weighted least-squares analysis that assumed the variance of velocity (v) to be a constant percentage of v for the entire data set. Then, in the weighted analysis, the slopes of these reciprocal plots were plotted according to the **4d** concentrations. Data analysis was performed with Graph Pad Prism 4.03 software (Graph Pad Software Inc.).

4.3.4. Molecular modelling

All calculations and analyses were carried out with Molecular Operating Environment (MOE) program (Chemical Computing Group, Montreal, Canada). The X-ray crystal structures of MAO-B (PDB code 2 V61) and MAO-A (PDB code 2Z5X) were applied to build the starting model, which were obtained from the Protein Data Bank (www.rcsb.org). Heteroatoms and water molecules in the PDB files were removed and all hydrogen atoms were subsequently added to the proteins. Compounds **4d** were drawn in MOE. Then the compound was protonated using the protonate 3D protocol and energy was minimized using the MMFF94x force field in MOE. After the enzymes and compounds were ready for the docking study, compounds were docked into the active site of the protein by the "Triangle Matcher" method. The dock scoring in MOE software was done using ASE scoring function and forcefield was selected as the refinement method. The 10 best positions of the molecule were retained and scored. After docking, the geometry of resulting complex was studied using the MOE's pose viewer utility.

4.3.5. Cell viability and neuroprotection activity assay

PC12 cells (rat pheochromocytoma) was obtained from the Cell Bank of the Chinese Academy of Sciences (Shanghai, China) and cultured in RPMI-1640 medium containing 10% (v/v) foetal bovine serum, 100 U penicillin/mL and 100 mg streptomycin/mL under 5% CO_2 at 37 °C. The culture media was replaced every other day. PC12 cells ($5*10^3$ cells/well) were cultured in 96-well plates and allowed to adhere and grow. Cells were placed into serum-free medium and treated with compounds after reached the required confluence. The survival of cells was determined by MTT assay after 24 h. The absorbance of each well was measured using a microculture plate reader with a test wavelength of 570 nm and a reference wavelength of 630 nm. Results were expressed as the mean ± SD of three independent experiments. PC12 cells ($5*10^3$ cells/well) were cultured in 96-well plates for neuroprotection activity assay. After 24 h, the medium was removed and replaced with the tested compounds (20 μM) at 37 °C and then incubated for another 24 h. Rasagiline was used as the control with the same concentration of 20 μM. Then, the cells were exposed to 6-OHDA (200 μM) and Rotenone (1.5 μM) respectively and incubated at 37 °C for 24 h before assayed with MTT. PC12 cells were cultured without test compound or neurotoxins as control groups and the results were expressed by percentage of control. Results were expressed as the mean ± SEM of three independent experiments.

4.3.6. In vitro blood–brain barrier permeation assay

Brain penetration of compounds was evaluated using a parallel artificial membrane permeation assay (PAMPA) in a similar manner as described by Di *et al* [37]. Commercial drugs were purchased from Sigma and Alfa Aesar. The porcine brain lipid (PBL) was obtained from Avanti Polar Lipids. The donor microplate (PVDF membrane, pore size (0.45 mm) and the acceptor microplate were both from Millipore. The 96-well UV plate (COSTAR$^{@}$) was from Corning Incorporated. The acceptor 96-well microplate was filled with 300 μL of PBS/EtOH (7: 3), and the filter membrane was impregnated with 4 μL of PBL in dodecane (20 mg/mL). Compounds were dissolved in DMSO at 5 mg/mL and diluted 50-fold in PBS/EtOH (7: 3) to achieve a concentration of 100 μg/

mL, 200 μL of which was added to the donor wells. The acceptor filter plate was carefully placed on the donor plate to form a sandwich construction, and kept undisturbed for 16 h at 25 °C. After incubation, the donor plate was carefully removed and the concentration of compound in the acceptor wells was determined using an UV plate reader (Flexstation@ 3). Every sample was analyzed at five wavelengths, in four wells, in at least three independent runs, and the results were expressed as the mean ± SD. In each experiment, 9 quality control standards of known BBB permeability were included to validate the analysis set.

4.3.7. Acute toxicity test [36]

All experimental procedures were conducted in accordance with the guidelines of Ethics Committee of Shanghai University of Traditional Chinese Medicine for the Care and Use of Laboratory Animals. Animals were randomly divided into two groups: control group and experimental group (2000 mg/kg, n = 10 per/group). Before treatment, animals were fasted overnight. Compound **4d** was suspended in 0.5% carboxymethyl cellulose sodium (CMC-Na) salt solution and orally administered according to the divided groups. Then feed and water were provided. After administration of **4d**, the mice were observed continuously for any abnormal behavior and mortality changes of mice were observed continuously in the first 4 h, intermittently in the next 24 h, and occasionally thereafter for 14 days for the onset of any delayed effects. All animals were sacrificed after being anaesthetized by ether on the 14th day after drug administration.

4.3.8. Animals and treatment

Male C57BL/6 mice (body weight: 23 ± 2 g, 10 weeks of age) were supplied by Shanghai Medical Laboratory Animal Center. Mice were kept in a room with 12 h light/dark cycles at 20–25 °C and 60% relative humidity for and obtained water and food ad libitum. Five groups of mice (n = 5/group) were distributed for this study. The groups were control, MPTP, rasagiline (standard), compound **4d** (5 mg/kg) and compound **4d** (10 mg/kg). In order to induce an acute experimental Parkinsonism, the mice were injected i.p. with 20 mg/kg MPTP hydrochloride, at 2 h intervals for altogether four injections in a day. In the coming three days, rasagiline (10 mg/kg) and compound **4d** (5 and 10 mg/kg) were administrated i.g. once a day.

4.3.9. Behavioral test

4.3.9.1. Hindlimb test. The mice were subjected to the hindlimb test as mentioned previously at 4th days after the final injection of MPTP. According to the position of their hindlimbs, the mice were suspended by grasping the tail and scored on a scale of 0–4. The basic score of each mouse is 4 points, from which the score of 1 point was deducted for each abnormal hindlimb movement of limbs or joints.

4.3.9.2. Rotarod test. The day before the experiment, mice were trained until they could stay on a rotarod (Zhenghua Biologic Apparatus Facilities, China) for 120 s without falling down. During the experiment, mice were placed on the rotary apparatus which started at 5 rpm for 20 *sec* and then accelerated to 25 rpm within 5 min. When the mouse dropped from the rotarod, each test would be finished and the length of time was recorded. Each animal was tested in three separate trials, and separated by one hour at a time.

Declaration of Competing Interest

The authors declared that there is no conflict of interest.

Acknowledgment

We gratefully acknowledge the financial support by programmes of the National Natural Science Foundation of China [grant numbers 81872981, 21807052]; The Key project of Shanghai 3-year plan [grant number ZY(2018-2020)-CCCX-2001-04]; The National Scientific and Technological Major Special Project of China [grant number 2019ZX09201004-002]; Shanghai Science and technology innovation project [17401901900]; The projects sponsored by the development fund for Shanghai talents [grant number 2018105]; Youth Talent Sail Plan from the Shanghai Committee of Science and Technology [grant number 18YF1423600]; Program of Shanghai Academic/Technology Research Leader [grant number 18XD1403700]; The projects sponsored by the development fund for Shanghai talents [grant number 2018105]; Outstanding Youth Talents in Jiangxi province [Grant No. 20192BCB23018]; Jiangxi University of Traditional Chinese Medicine 1050 Youth Talent Project [Grant No. 1141900616].

Appendix A. Supplementary data

Supplementary data to this article can be found online at https://doi.org/10.1016/j.bioorg.2021.104685.

References

[1] J.P.M. Finberg, J. Wang, K. Bankiewicz, J. Harvey-White, I.J. Kopin, D. S. Goldstein, Increased striatal dopamine production from L-DOPA following selective inhibition of monoamine oxidase B by R(+)-N-propargyl-1-aminoindan (rasagiline) in the monkey, J. Neural Transmission-Supplement (1998) 279–285.
[2] W. Dauer, S. Przedborski, Parkinson's disease: Mechanisms and models, Neuron 39 (2003) 889–909.
[3] A. Carlsson, Treatment of Parkinson's with L-DOPA. The early discovery phase, and a comment on current problems, J. Neural Transm. 109 (2002) 777–787.
[4] D.J. Pedrosa, L. Timmermann, Review: management of Parkinson's disease, Neuropsychiatr. Dis. Treat. 9 (2013) 321–340.
[5] R. Talati, W.L. Baker, A.A. Patel, K. Reinhart, C.I. Coleman, Adding a dopamine agonist to preexisting levodopa therapy vs. levodopa therapy alone in advanced Parkinson's disease: a meta analysis, Int. J. Clin. Pract. 63 (2009) 613–623.
[6] S.K. Jha, N.K. Jha, D. Kumar, R.K. Ambasta, P. Kumar, Linking mitochondrial dysfunction, metabolic syndrome and stress signaling in Neurodegeneration, Biochimica Et Biophysica Acta-Molecular Basis of Disease 2017 (1863) 1132–1146.
[7] A. Nicotra, F. Pierucci, H. Parvez, O. Senatori, Monoamine oxidase expression during development and aging, Neurotoxicology 25 (2004) 155–165.
[8] M.B.H. Youdim, D. Edmondson, K.F. Tipton, The therapeutic potential of monoamine oxidase inhibitors, Nat. Rev. Neurosci. 7 (2006) 295–309.
[9] J.P.M. Finberg, Update on the pharmacology of selective inhibitors of MAO-A and MAO-B: Focus on modulation of CNS monoamine neurotransmitter release, Pharmacol. Ther. 143 (2014) 133–152.
[10] J. Jankovic, W. Poewe, Therapies in Parkinson's disease, Curr. Opin. Neurol. 25 (2012) 433–447.
[11] P.B. Huleatt, M.L. Khoo, Y.Y. Chua, T.W. Tan, R.S. Liew, B. Balogh, R. Deme, F. Goeloencser, K. Magyar, D.P. Sheela, H.K. Ho, B. Sperlagh, P. Matyus, C.L. L. Chai, Novel Arylalkenylpropargylamines as Neuroprotective, Potent, and Selective Monoamine Oxidase B Inhibitors for the Treatment of Parkinson's Disease, J. Med. Chem. 58 (2015) 1400–1419.
[12] A.C. Tripathi, S. Upadhyay, S. Paliwal, S.K. Saraf, Privileged scaffolds as MAO inhibitors: Retrospect and prospects, Eur. J. Med. Chem. 145 (2018) 445–497.
[13] A. Fonseca, M.J. Matos, J. Reis, Y. Duarte, M. Gutierrez, L. Santana, E. Uriarte, F. Borges, Exploring coumarin potentialities: development of new enzymatic inhibitors based on the 6-methyl-3-carboxamidocoumarin scaffold, RSC Adv. 6 (2016) 49764–49768.
[14] M.J. Matos, C. Teran, Y. Perez-Castillo, E. Uriarte, L. Santana, D. Vina, Synthesis and Study of a Series of 3-Arylcoumarins as Potent and Selective Monoamine Oxidase B Inhibitors, J. Med. Chem. 54 (2011) 7127–7137.
[15] C. Gnerre, M. Catto, F. Leonetti, P. Weber, P.A. Carrupt, C. Altomare, A. Carotti, B. Testa, Inhibition of monoamine oxidases by functionalized coumarin derivatives: Biological activities, QSARs, and 3D-QSARs, J. Med. Chem. 43 (2000) 4747–4758.
[16] F. Chimenti, D. Secci, A. Bolasco, P. Chimenti, B. Bizzarri, A. Granese, S. Carradori, M. Yanez, F. Orallo, F. Ortuso, S. Alcaro, Synthesis, Molecular Modeling, and Selective Inhibitory Activity against Human Monoamine Oxidases of 3-Carboxamido-7-Substituted Coumarins, J. Med. Chem. 52 (2009) 1935–1942.
[17] J.-S. Lan, Y. Liu, J.-W. Hou, J. Yang, X.-Y. Zhang, Y. Zhao, S.-S. Xie, Y. Ding, T. Zhang, Design, synthesis and evaluation of resveratrol-indazole hybrids as novel monoamine oxidases inhibitors with amyloid-beta aggregation inhibition, Bioorg. Chem. 76 (2018) 130–139.
[18] J.-S. Lan, Y. Ding, Y. Liu, P. Kang, J.-W. Hou, X.-Y. Zhang, S.-S. Xie, T. Zhang, Design, synthesis and biological evaluation of novel coumarin-N-benzyl pyridinium hybrids as multi-target agents for the treatment of Alzheimer's disease, Eur. J. Med. Chem. 139 (2017) 48–59.
[19] J.-S. Lan, T. Zhang, Y. Liu, Y. Zhang, J.-W. Hou, S.-S. Xie, J. Yang, Y. Ding, Z.-Z. Cai, Synthesis and evaluation of small molecules bearing a benzyloxy substituent as novel and potent monoamine oxidase inhibitors, Medchemcomm 8 (2017) 471–478.

[20] L.J. Legoabe, A. Petzer, J.P. Petzer, 2-acetylphenol analogs as potent reversible monoamine oxidase inhibitors, Drug Design Development and Therapy 9 (2015) 3635–3644.
[21] J.-S. Lan, S.-S. Xie, M. Huang, Y.-J. Hu, L.-Y. Kong, X.-B. Wang, Chromanones: selective and reversible monoamine oxidase B inhibitors with nanomolar potency, Medchemcomm 6 (2015) 1293–1302.
[22] L.J. Legoabe, A. Petzer, J.P. Petzer, alpha-Tetralone derivatives as inhibitors of monoamine oxidase, Bioorg. Med. Chem. Lett. 24 (2014) 2758–2763.
[23] L.J. Legoabe, A. Petzer, J.P. Petzer, Selected C7-substituted chromone derivatives as monoamine oxidase inhibitors, Bioorg. Chem. 45 (2012) 1–11.
[24] L.J. Legoabe, A. Petzer, J.P. Petzer, Inhibition of monoamine oxidase by selected C6-substituted chromone derivatives, Eur. J. Med. Chem. 49 (2012) 343–353.
[25] B. Strydom, J.J. Bergh, J.P. Petzer, Inhibition of monoamine oxidase by phthalide analogues, Bioorg. Med. Chem. Lett. 23 (2013) 1269–1273.
[26] L. Meiring, J.P. Petzer, A. Petzer, Inhibition of monoamine oxidase by 3,4-dihydro-2(1H)-quinolinone derivatives, Bioorg. Med. Chem. Lett. 23 (2013) 5498–5502.
[27] B. Schmidt, F. Wolf, C. Ehlert, Systematic Investigation into the Matsuda-Heck Reaction of alpha-Methylene Lactones: How Conformational Constraints Direct the beta-H-Elimination Step, J. Org. Chem. 81 (2016) 11235–11249.
[28] S.-S. Xie, X. Wang, N. Jiang, W. Yu, K.D.G. Wang, J.-S. Lan, Z.-R. Li, L.-Y. Kong, Multi-target tacrine-coumarin hybrids: Cholinesterase and monoamine oxidase B inhibition properties against Alzheimer's disease, Eur. J. Med. Chem. 95 (2015) 153–165.
[29] N.T. Tzvetkov, S. Hinz, P. Kueppers, M. Gastreich, C.E. Mueller, Indazole- and Indole-5-carboxamides: Selective and Reversible Monoamine Oxidase B Inhibitors with Subnanomolar Potency, J. Med. Chem. 57 (2014) 6679–6703.
[30] S.-Y. Li, N. Jiang, S.-S. Xie, K.D.G. Wang, X.-B. Wang, L.-Y. Kong, Design, synthesis and evaluation of novel tacrine rhein hybrids as multifunctional agents for the treatment of Alzheimer's disease, Org. Biomol. Chem. 12 (2014) 801–814.
[31] D. Tao, Y. Wang, X.-Q. Bao, B.-B. Yang, F. Gao, L. Wang, D. Zhang, L. Li, Discovery of coumarin Mannich base derivatives as multifunctional agents against monoamine oxidase B and neuroinflammation for the treatment of Parkinson's disease, Eur. J. Med. Chem. 173 (2019) 203–212.
[32] W. Li, X. Yang, Q. Song, Z. Cao, Y. Shi, Y. Deng, L. Zhang, Pyridoxine-resveratrol hybrids as novel inhibitors of MAO-B with antioxidant and neuroprotective activities for the treatment of Parkinson's disease, Bioorg. Chem. 97 (2020).
[33] Z. Wang, J. Wu, X. Yang, P. Cai, Q. Liu, K.D.G. Wang, L. Kong, X. Wang, Neuroprotective effects of benzyloxy substituted small molecule monoamine oxidase B inhibitors in Parkinson's disease, Bioorg. Med. Chem. 24 (2016) 5929–5940.
[34] H. van de Waterbeemd, E. Gifford, ADMET in silico modelling: Towards prediction paradise? Nat. Rev. Drug Discovery 2 (2003) 192–204.
[35] http://www.molinspiration.com/services/properties.html (accessed August 2016).
[36] W.A. Pardridge, Alzheimer's disease drug development and the problem of the blood-brain barrier, Alzheimers Dementia 5 (2009) 427–432.
[37] J.J. Braymer, A.S. Detoma, J.-S. Choi, K.S. Ko, M.H. Lim, Recent Development of Bifunctional Small Molecules to Study Metal-Amyloid-beta Species in Alzheimer's Disease, Int. J. Alzheimer's Disease 2010 (2011).
[38] C. Lu, Y. Guo, J. Yan, Z. Luo, H.-B. Luo, M. Yan, L. Huang, X. Li, Design, Synthesis, and Evaluation of Multitarget-Directed Resveratrol Derivatives for the Treatment of Alzheimer's Disease, J. Med. Chem. 56 (2013) 5843–5859.
[39] M.-H. Nam, M. Park, H. Park, Y. Kim, S. Yoon, V.S. Sawant, J.W. Cho, J.-H. Park, K. D. Park, S.-J. Min, C.J. Lee, H. Chooaii, Indole-Substituted Benzothiazoles and Benzoxazoles as Selective and Reversible MAO-B Inhibitors for Treatment of Parkinson's Disease, ACS Chem. Neurosci. 8 (2017) 1519–1529.
[40] S.Y. Woo, J.H. Kim, M.K. Moon, S.-H. Han, S.K. Yeon, J.W. Choi, B.K. Jang, H. J. Song, Y.G. Kang, J.W. Kim, J. Lee, D.J. Kim, O. Hwang, K.D. Park, Discovery of Vinyl Sulfones as a Novel Class of Neuroprotective Agents toward Parkinson's Disease Therapy, J. Med. Chem. 57 (2014) 1473–1487.
[41] J.Y. Chung, J.W. Lee, C.H. Ryu, H.K. Min, Y.J. Yoon, M.J. Lim, C.H. Park, 1- 2-(4-Benzyloxyphenoxy)Ethyl Imidazole inhibits monoamine oxidase B and protects against neuronal loss and behavioral impairment in rodent models of Parkinson's disease, J. Neurosci. Res. 93 (2015) 1267–1278.